VOYAGER PLANETARY RADIO ASTRONOMY EXPERIMENT OBSERVATIONS: PLASMA WAVES IN THE JOVIAN AND SATURNIAN MAGNETOSPHERES

B. M. Pedersen*

Abstract

During the two Jupiter – and the following two Saturn – Voyager encounters, the Planetary Radio Astronomy experiment detected in–situ plasma waves inside the two planetary magnetospheres. We review the different kinds of observed waves and then briefly discuss their excitation mechanisms, as well as their possible role for generating observed magnetospheric radio emissions.

1 Introduction

During the passages through the Jovian and Saturnian magnetospheres, the Planetary Radio Astronomy (PRA) experiments (Warwick et al., 1977) on the Voyager 1 and 2 spacecraft detected different kinds of local plasma wave phenomena (Warwick et al., 1979a, 1979b, 1981, 1982).

These in–situ observations of electrostatic waves can be considered as a by–product of the PRA–experiments, principally designed to observe radio emissions from planetary magnetospheres, in general at higher frequencies.

However, the study of such magnetospheric plasma waves is important, as their characteristics can give informations about the electron densities, the temperatures and in some cases the distribution functions at specific places within the magnetosphere. The positions of such waves suggest potential source locations for the radio emissions.

Hence, observations of magnetospheric plasma waves give important informations for understanding the physical processes, taking place within a planetary magnetosphere.

*Paris-Meudon Observatory, Laboratoire Associe du CNRS 324, 92195 Meudon Principal CEDEX, France.

2 Observations

Many plasma wave phenomena within the Jovian and Saturnian magnetospheres were only detected by the Voyager Plasma Wave (PWS) experiments (Scarf and Gurnett, 1977), operating at low frequencies ($\leq$ 56 kHz). However, at several occasions, the higher frequency range and/or the high frequency resolution of the PRA–experiment have played an important role for interpreting the true nature and the evolution of the electrostatic waves along the spacecraft trajectory within the magnetospheres.

2.1 Observations near Jupiter

An overview of the plasma waves near Jupiter, as observed by the Voyager spacecraft, is found in Gurnett and Scarf (1983). Here we shall only comment on the electrostatic waves, observable above the low–frequency limit $\sim$ 20 kHz of the PRA experiment.

2.1.1 Plasma Waves Within the Io Plasma Torus

Around closest approach to Jupiter, when Voyager 1 during inbound – and outbound – pass traversed the Io plasma torus (IPT), strong modulation patterns appeared at low frequencies on the PRA–dynamic spectrum along a varying plasma line as shown in Figure 1.

For a thorough discussion of these observations we refer the reader to Birmingham et al. (1981). A detailed study of the LF–fixed frequency plots (presented on Figure 2 together with corresponding gyroharmonics as derived from the magnetometer experiment measurements) has allowed to determine the variation of the cold upper hybrid resonance frequency (identified as intense impulsive emissions) through the IPT. Figure 3 shows the corresponding density plot of the cold electron component as function of time. From the smooth curves we deduced the model of electron density shown in Figure 4. This idealized model was constructed under the assumption of an azimuthal symmetry with respect to Jupiter's magnetic axis and a symmetry with respect to the particle centrifugal equator.

The modulation pattern, accompanying most of the time the upper hybrid resonance frequency line in Figure 1, is due to electrostatic gyroharmonic waves at $(n + 1/2)f_{ce}$ above and/or below f_{uH} (f_{ce} and f_{uH} are respectively the electron cyclotron – and the upper hybrid resonance frequency). Figure 2 shows clearly these $(n + 1/2)f_{ce}$ – waves, characterized by weak, smooth emission humps between the indicated gyroharmonics. On Figure 4 the positioning of these auxiliary plasma waves relative to the f_{uH}–line is indicated at each location along the spacecraft trajectory. As we shall mention below, this positioning is significant for determining the plasma parameters.

2.1.2 Plasma Waves in the Vicinity of the Magnetic Equatorial Plane

Figure 5 shows the two Voyager trajectories close to Jupiter with respect to the magnetic equatorial plane (MEP). Due to the magnetic dipole tilt relative to the rotation–axis

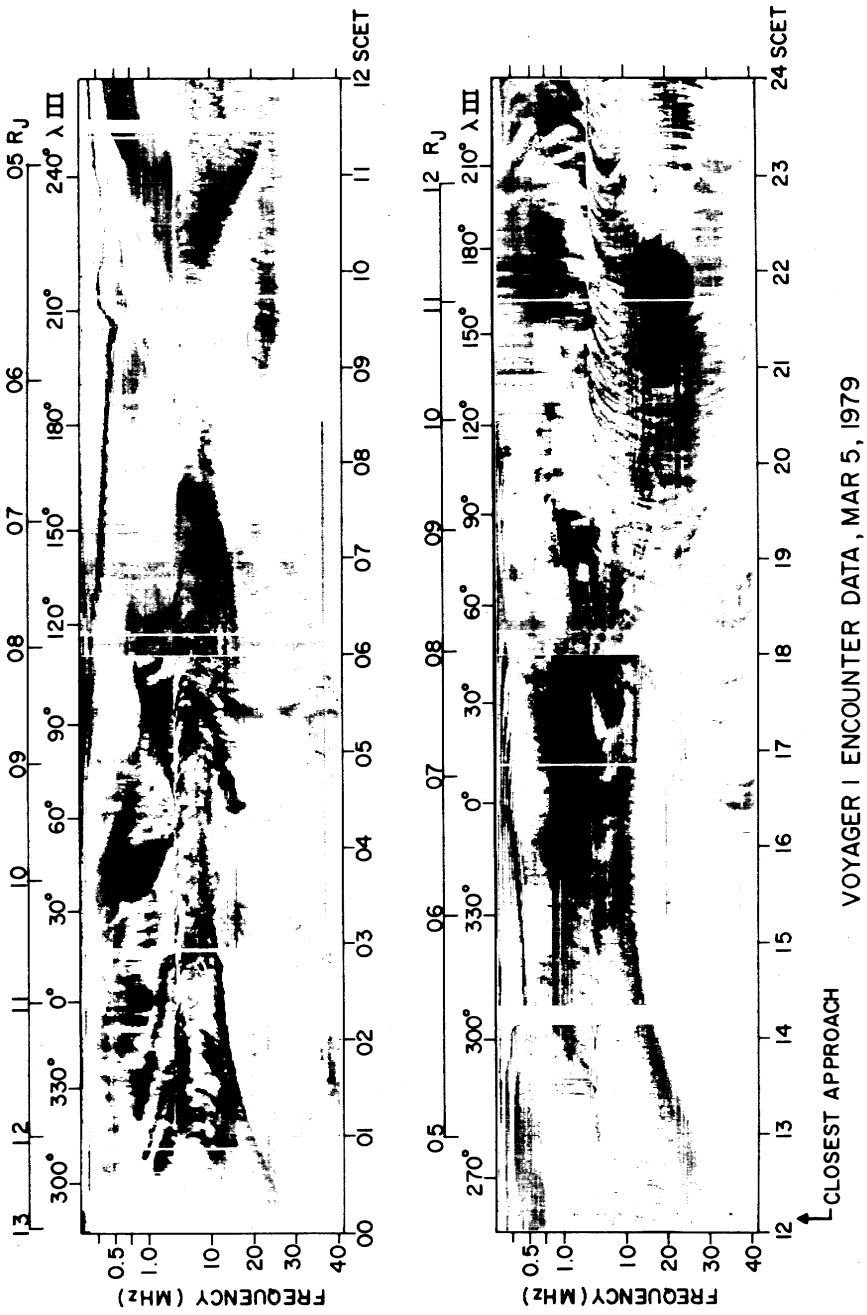

Figure 1: Dynamic spectrum of Jupiter's radio emissions and local plasma waves observed by the PRA–experiment on Voyager 1 around closest approach to Jupiter. The total received power in each of the 198 frequency channels is shown as a function of time and sub–Voyager Jovian longitude. Increasing total power is indicated by increasing darkness. (G.S.F.C. document).

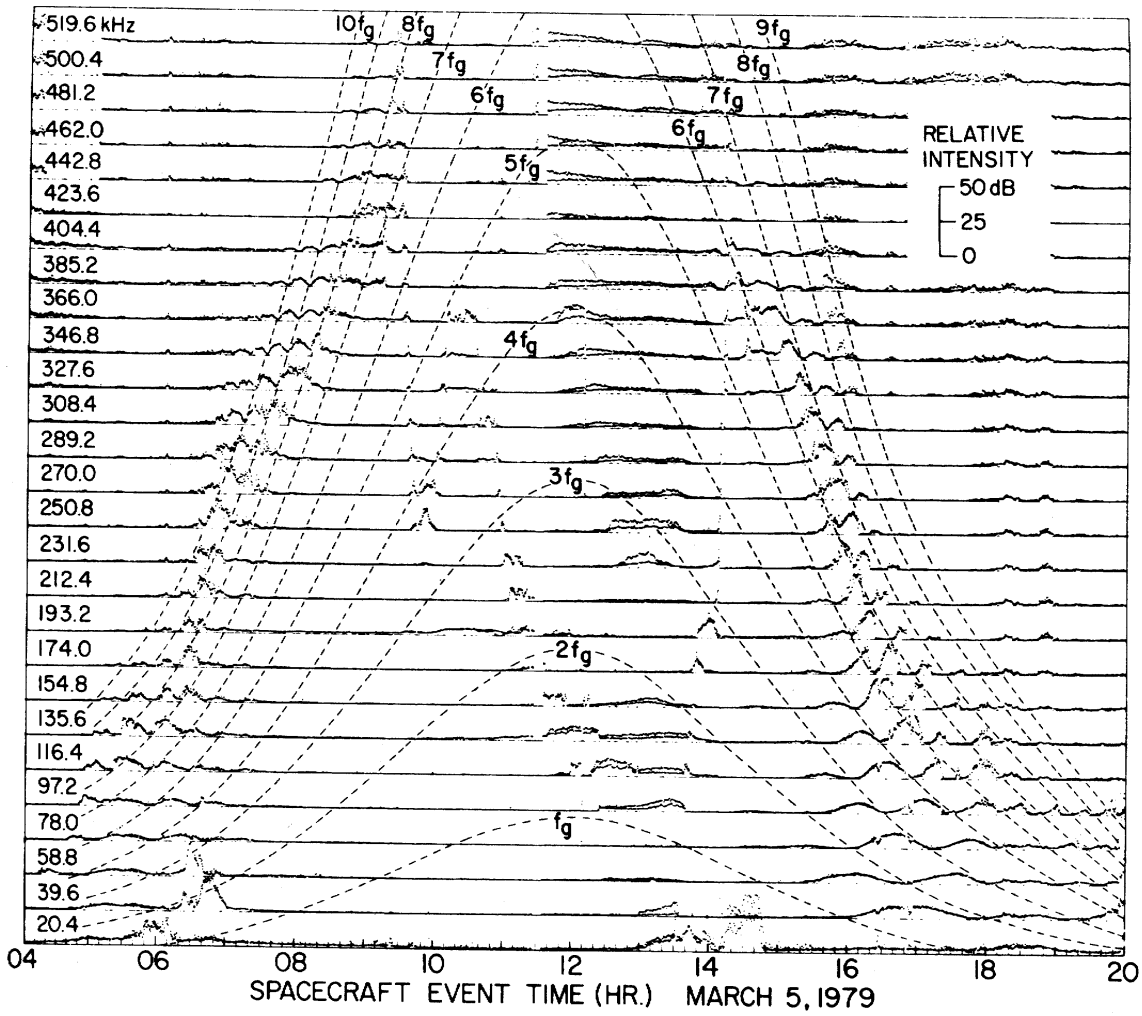

Figure 2: Intensity–time tracings of gyroharmonic lines in the IPT. Within each trace, identified by its frequency in kHz, the vertical dimension is logarithmically proportional to intensity. The variation in time of the electron gyrofrequency and its first nine integral harmonics is shown superposed (from Birmingham et al., 1981).

the MEP is crossed twice during each planetary rotation by a spacecraft, going round Jupiter at low latitudes. During many of these crossings close to Jupiter ($< 15R_J$), the PRA–experiments detected electrostatic (i.e. unpolarized) waves at positions along the spacecraft trajectories close to or around the passages of the MEP.

Table 1 gives the detailed characteristics for each passage, where the PRA–instrument observed these particular emissions. Table 2 sums up the essential characteristics of the plasma waves, observed during each event, and Figure 6 shows fixed frequency plots for some typical events.

Figure 7 illustrates the locations, where the emissions are detected. They are confined to a layer outside the torus, situated around the MEP with a thickness of $\sim 0.5R_J$ perpendicular to the MEP.

A detailed examination of the spectral density as a function of frequency–channels demon-

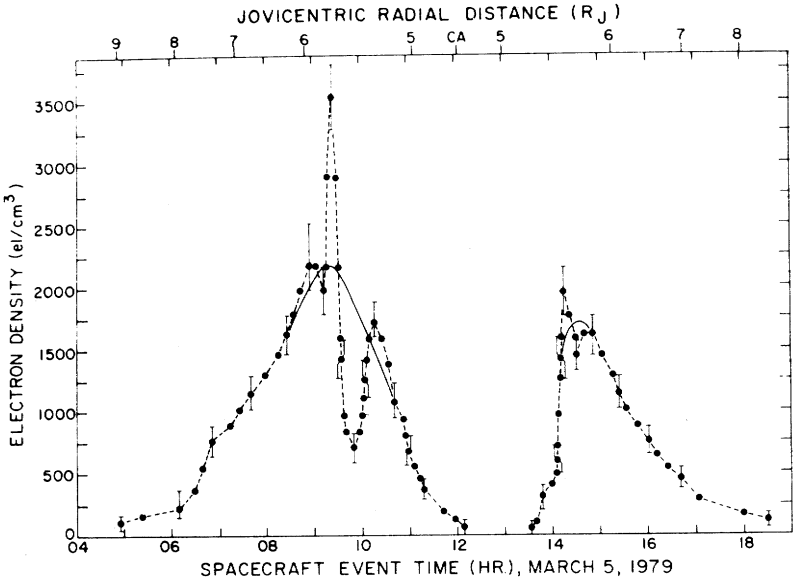

Figure 3: Plot of the density of the cold electron component of the IPT as a function of time derived from PRA measurements of the cold upper hybrid resonance frequency and magnetometer measurements of the electron gyrofrequency (from Birmingham et al., 1981).

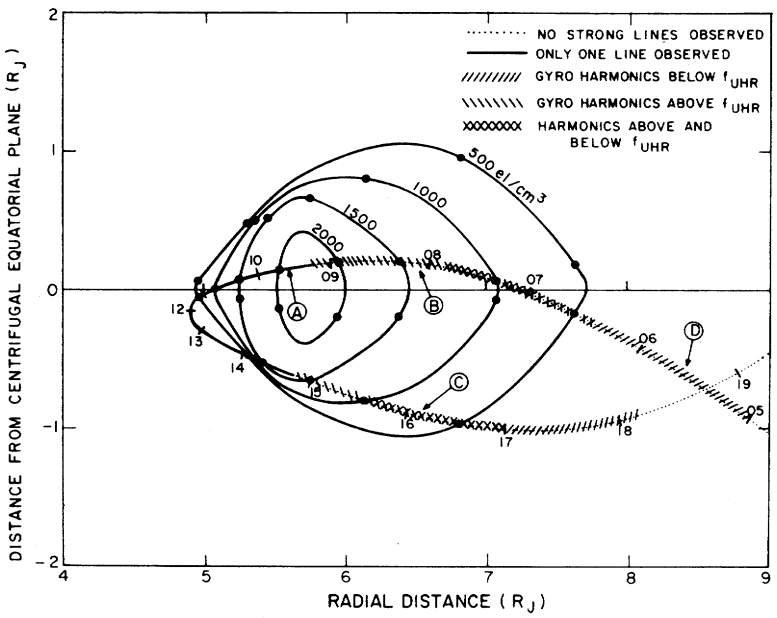

Figure 4: A model of the average density distribution in a meridional plane for the cold electron component of the IPT. The projection of the Voyager 1 trajectory is coded to indicate the locations at which various classes of plasma wave lines were detected by the PRA instrument (from Birmingham et al., 1981).

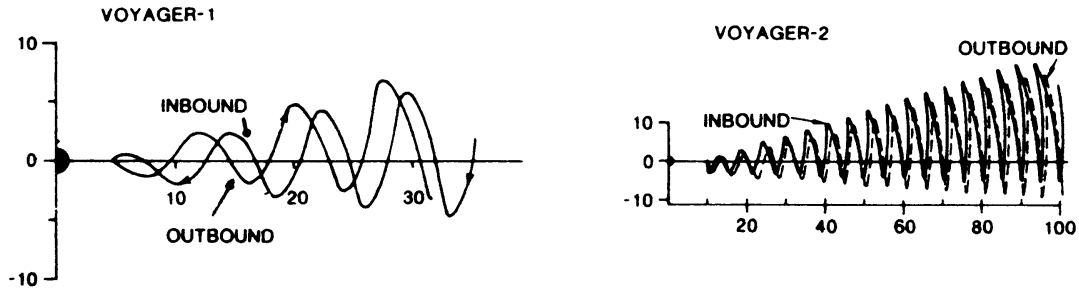

Figure 5: Meridian plane projections with respect to Jovian magnetic equator for the trajectories of Voyager 1 and 2 close to the planet (from Scarf et al., 1983).

	Date and Hour	Jovicentric radial distance (R_J)	Gyrofrequency $\approx f_{ce}$ (kHz)	Plasma Characteristics $n_e(cm^{-3})$	T_e(ev)	$n_H\ T_H/n_cT_c$
VOYAGER 1 A:	79 - 03 - 05 0h	12.8	4	10 (4)	40 (4)	
B:	79 - 03 - 05 6h30	7.5	24	400 (1)	90 (2)	0.7 (2)
C:	79 - 03 - 05 20h10	9.8	10	≥40 (3)		
VOYAGER 2 D:	79 - 07 - 09 9h40	13.8	3	10 (4)	60 (4)	
E:	79 - 07 - 09 13h30	12.1	5	10 (4)		
F:	79 - 07 - 09 22h	10.1	9	30 (4)		
G:	79 - 07 - 10 0h	10.1	9	50 (4)		
H:	79 - 07 - 10 9h10	13	4	15 (2)	150 (2)	3 (2)
I:	79 - 07 - 10 12h20	14.7	3	2 (2)	350 (2)	1 (2)

(1) Warwick et al., 1979a; (2) Scudder et al., 1981; (3) E. Siddler (private comm.); (4) Mc Nutt et al., 1981.

Table 1: Characteristics for Jovian magnetic equatorial crossings

strates that all events except event B show highest intensity in a channel close to the calculated $f_{uH} = \left[f_{ce}^2 + f_{pe}^2\right]^{1/2}$, where f_{pe} (kHz) $= 9\ [n_e(\mathrm{cm}^{-3})]^{1/2}$. In all events $f_{pe} \gg f_{ce}$.

During the event F, taking place at 10.1 R_J, an impulsive, very intense emission – one of the strongest emissions ever recorded by the PRA–instruments – saturated very often the 59 kHz–channel, i.e. showed a spectral density higher than 10^{-10} V^2 M^{-2} Hz^{-1}.

Plasma waves, tightly confined to the Jovian magnetic equator, were already reported by Kurth et al. (1980). The lower frequency range of the PWS instrument allowed to observe emissions with narrow–band features out to distances of about 23 R_J. By analogy with observations of electron–cyclotron harmonic waves, confined to the geomagnetic equator in the Earth's magnetosphere (see for example Gough et al., 1979), Kurth et al. suggested that these plasma waves are $(n + 1/2)f_{ce}$ – emissions, extending from just above f_{ce} up

		Date and Hour	Duration: R_J perpendicular to the magnetic equator at 20.4 kHz	Duration: R_J perpendicular to the magnetic equator at f_{max}(kHz)	Maximum frequency f_{max}(kHz)	Frequency at Max. spectral density (kHz)	Max. Spectral density $V^2\ m^{-2}\ Hz^{-1}$
VOYAGER 1	A:	79 - 03 - 05 0h	0.6	0.08	136	20	10^{-12}
	B:	79 - 03 - 05 6h30	0.5 + 0.25	0.17	212	59	10^{-12}
	C:	79 - 03 - 05 20h10	0.3 + 0.1	0.15	212	78	10^{-10}
VOYAGER 2	D:	79 - 07 - 09 9h40	0.12	0.6	59	40	10^{-11}
	E:	79 - 07 - 09 13h30	0.6	0.3	78	40	2.10^{-11}
	F:	79 - 07 - 09 22h	0.3	0.1	78	59	10^{-10}
	G:	79 - 07 - 10 0h	0.5	0.2	78	59	7.10^{-12}
	H:	79 - 07 - 10 9h10	0.3	0.1	78	78	2.10^{-13}
	I:	79 - 07 - 10 12h20	0.45	0.17	78	20	10^{-10}

Table 2: Characteristics of plasma waves near magnetic equatorial plane

to f_{uH}.

As the PRA–channels are spaced at 19.2 kHz intervals – most often much larger than the local gyrofrequency – the narrow–banded character of the emissions does not show up on the PRA–spectra.

2.2 Observations near Saturn

A general description of plasma waves in the Saturnian system is given in Scarf et al. (1984). More detailed discussions can be found in Scarf et al. (1983) and Kurth et al. (1983).

The PRA–observations during the Voyager–Saturn encounters (Kaiser et al., 1984) were dominated by the Saturnian Kilometric Radiation (SKR) except during closest approach, where the Saturn Electrostatic Discharges (SED) were detected during a few days.

Generally, the SKR extends down to very low frequencies (60–80 kHz). However, during the Voyager 1 – ring plane crossing nearest to the planet (see Figure 8), the SKR was only present above $\sim$ 120 kHz, and during the unique Voyager 2 – ring plane event the SKR was absent. Consequently, the low frequency phenomena taking place during these periods were not masked by the SKR. But before describing in detail the plasma waves observed close to the ring plane, we shall briefly summarize the PRA–observations during the Voyager l Titan flyby.

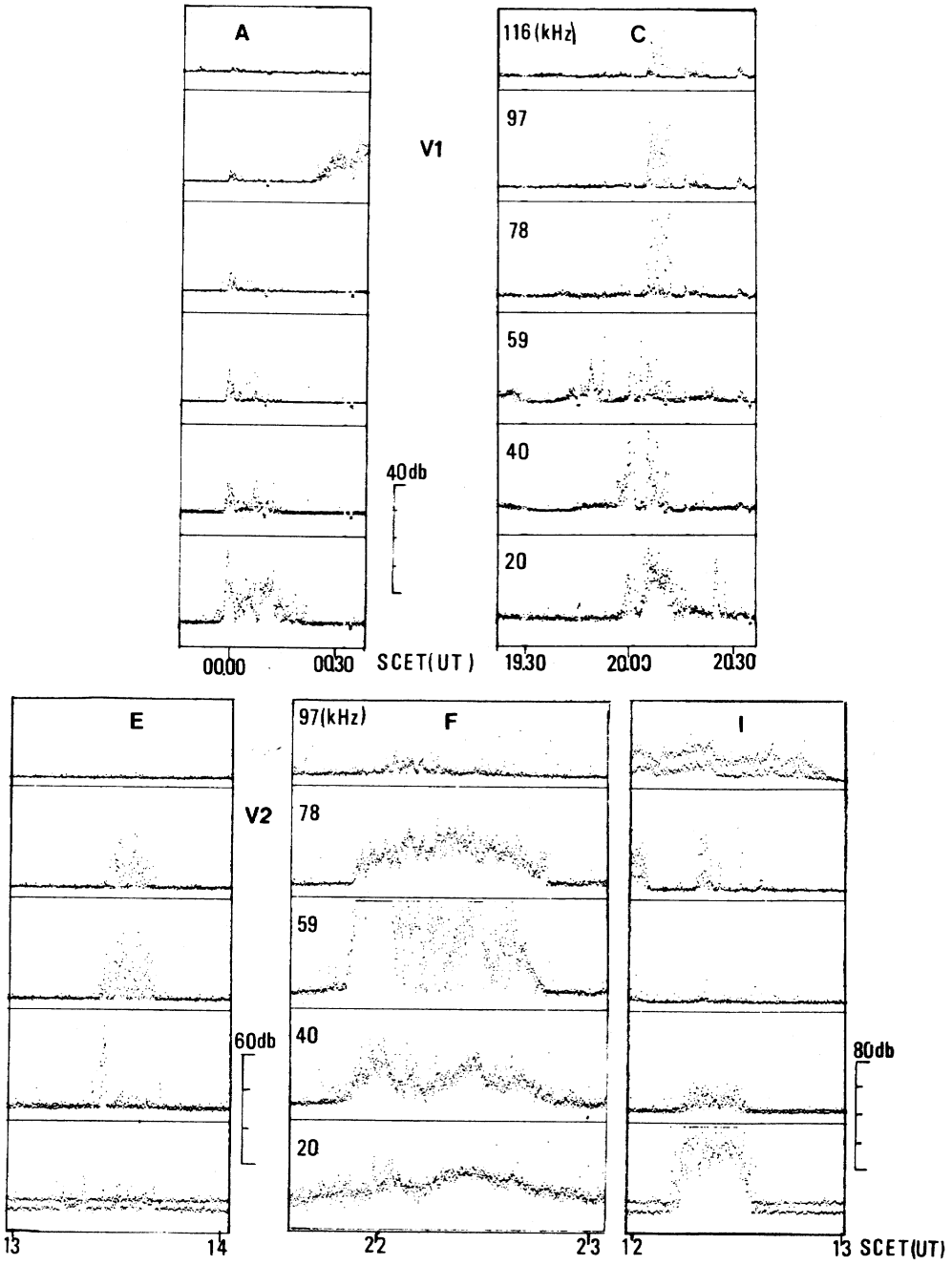

Figure 6: PRA–fixed frequency intensity plots for most typical events in Tables 1 and 2

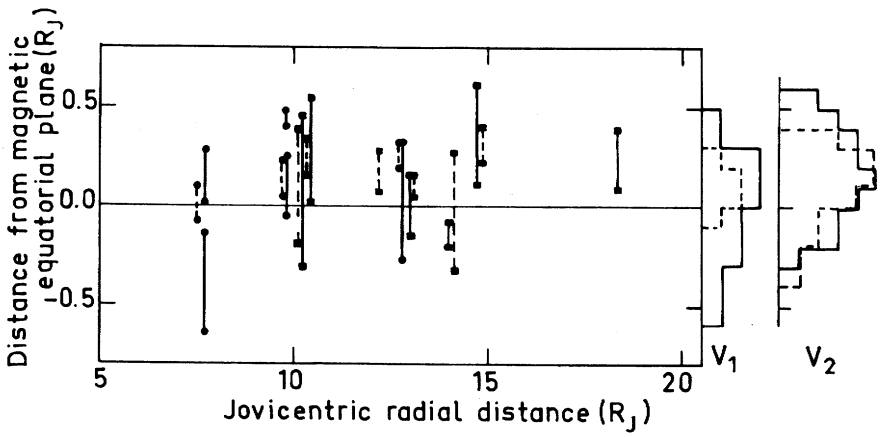

Figure 7: Thickness and position of the IPT–tail as detected by the two Voyager (dots: V1, fullboxes: V2) under the assumption that the observed emissions limit the tail–region. Full and dotted lines refer to emissions at 20 kHz and at observed maximum frequency. The histogram shows the positions for all measured emissions.

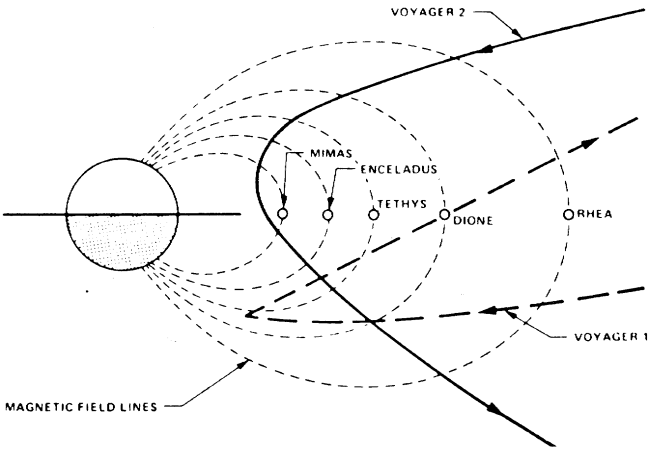

Figure 8: Meridian plane projections of Voyager 1 and 2 trajectories around closest approach to Saturn.

2.2.1 Plasma Waves Observed Within Titan's magnetospheric Wake

The PRA–observations during the Voyager 1 Titan flyby have been described in detail in Daigne et al. (1982). A general overview of Titan's magnetospheric interaction is given in Neubauer et al. (1984).

During the Voyager 1 – Titan flyby, Titan was located within the Saturnian magnetosphere. In this case, the rotating magnetospheric plasma of Saturn sweeps over the moon with a nominal velocity of about 200 km/sec, generating a magnetospheric wake.

Figure 9a shows the spacecraft trajectory relative to an idealized magnetospheric wake structure. Figure 9b presents the PRA low frequency plots for the flyby period. We point out two conspicuous features on these plots, the spiky bursts and the drop outs, i.e. intervals without emission.

Comparing with the magnetometer data, the spikes have been interpreted as electrostatic waves, occurring at the local upper hybrid resonance, at the inbound– (59 kHz, 0538:53) and at the outbound– (39 and 20 kHz, from 0543:29 to 0543:53) crossings of Titan's induced tail (Daigne et al., 1982). Hence we obtain maximum densities of ~ 40 cm^{-3} and ~ 20 cm^{-3}, respectively, at the inbound– and at the outbound–edge of the wake.

In Figure 9b the emission in the 39, 59 and 78 kHz channels which starts around 05:43, when Voyager exits the wake, was first interpreted as an independent radio emission from Titan. But we (Daigne et al., 1982) compared the overall emission pattern, shown in Figure 9, with the SKR – pattern for the three preceding Saturn rotations and with the corresponding Voyager 2 – pattern and ruled out this possibility. The emission during the Titan flyby was normal low frequency SKR, but during the drop outs perturbed by propagation effects in enhanced density regions with Titan's induced magnetic tail.

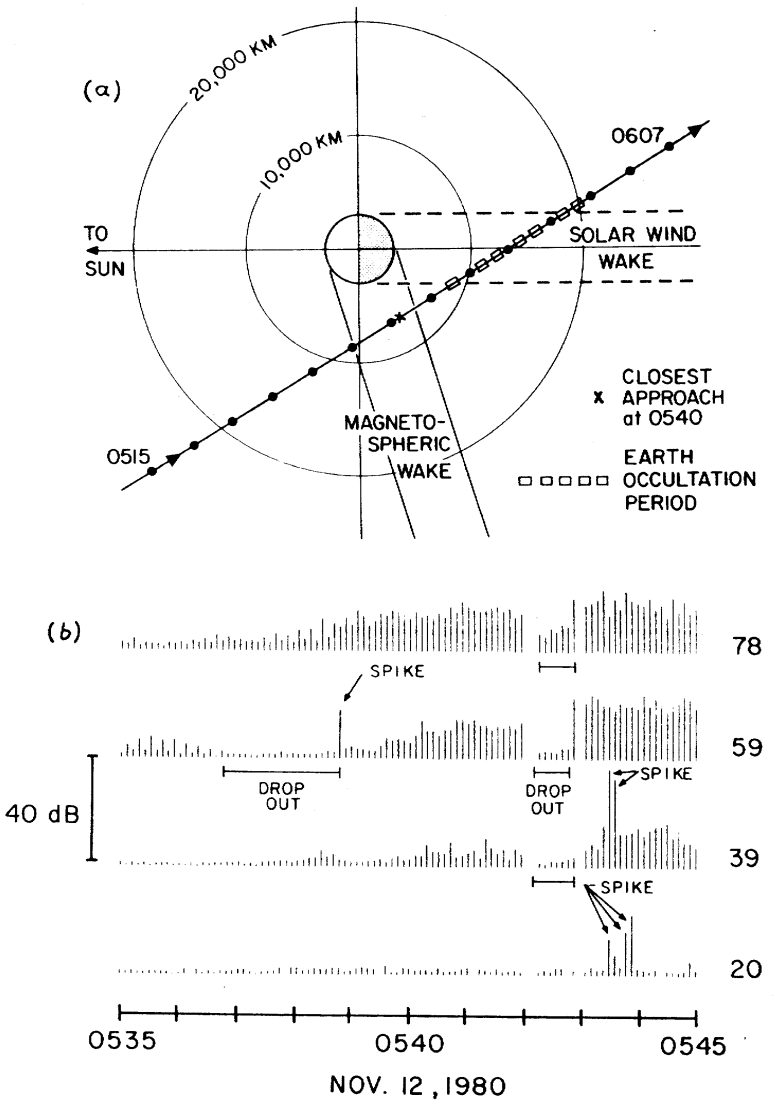

Figure 9: (a) Voyager 1 trajectory with respect to Titan's magnetospheric wake. Black dots indicate 4 min. – intervals. (b) PRA–fixed LF frequency plots around closest Titan fly–by (from Daigne et al., 1982).

2.2.2 Plasma Waves Observed Around the Saturnian Ring Plane

During the inbound Voyager 1 – ring plane crossing close to Titan, no evidence for plasma waves showed up on the PRA–spectrum, perhaps due to the low frequency SKR–component, as mentioned above.

The outbound Voyager 1 crossed the ring plane at the orbit of Dione and the Voyager 2 passed the ring plane just outside the G–ring.

Figure 10 shows the low frequency PRA–observation around the Voyager 1 ring plane crossing. We commented on this spectrum in detail in Pedersen et al. (1981). The broad banded emission (triangle signature) around the ring plane crossing (RC) is electron – and ion shot noise as shown by Aubier et al. (1983). The electromagnetic (polarized) emissions (1) and (2), preceding the RC, are respectively interpreted as VLF–emission ($f < f_{pe}$ and $f < f_{ce}$) and Saturnian non–thermal continuum radiation, analogous to the component, observed in the terrestrial magnetosphere (Kurth et al., 1981).

Plasma waves were identified below 60 kHz around the ring plane. A varying pattern of gyroharmonics above the upper hybrid resonance was determined as already described for Figure 2. Brief spiky bursts (•) were identified as waves at f_{uH}, whereas smooth emission humps of longer duration (×), situated between the gyroharmonics as deduced from magnetometer data, were classified as accompanying $(n + 1/2)f_{ce}$ harmonic waves. The varying frequency of the electrostatic noise at f_{uH} allows a direct estimate of the electron density around RC ($4 < R < 7R_S$), varying from about 1 el/cm^3 outside the ring plane to $\sim$ 20 el/cm^3 at RC. This result has been confirmed by the plasma science experiment (Scarf et al., 1984).

The emissions observed by the PRA–instrument during the unique Voyager 2 ring plane crossing (see Figure 8) are shown in Figure 11. The broad banded ring plane noise has been explained as grain shot noise, induced on the spacecraft body and the radio astronomy antennas (Aubier et. al., 1983). By analogy with the Voyager 1 ring plane event we have interpreted the unpolarized waves around the ring plane in the lowest PRA–channels as $(n + 1/2)f_{ce}$ – gyroharmonics (Warwick et al., 1982).

3 Discussion

Birmingham et al. (1981) attribute the plasma waves observed in the Io plasma torus to the instability of a plasma, consisting of a "cold" background plasma and a "hot" component. Free energy for the instability derives from a loss cone distribution of the hot electrons, while the cold plasma provides a dielectric background, on which the unstable modes develop.

The position of the $(n + 1/2)f_{ce}$ emissions relative to f_{uh} along the Voyager trajectory is an indicator of the cold to hot electron temperature ratio. The instability calculations by Birmingham et al. indicate for the observations within the Io plasma torus (Figure 2) that in addition to the cold plasma being much more dense than the hot, the temperature ratio of cold and hot components T_C/T_H is increased by a factor of 4 in passing from the

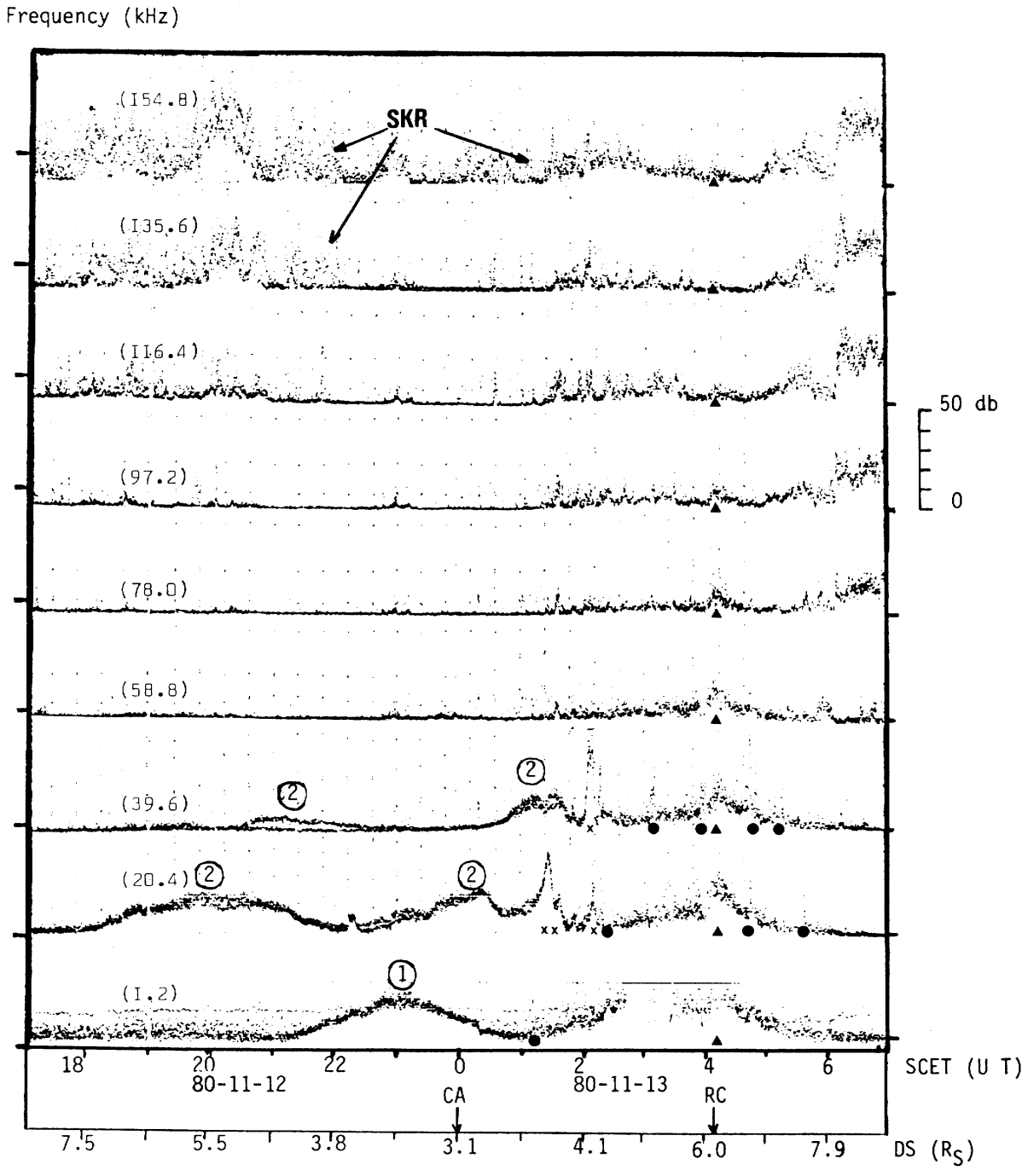

Figure 10: Fixed frequency plots (intensity in dB μV^{-1} kHz^{-1}) of the lowest PRA frequencies as a function of the distance (D_S) from Saturn. CA denotes the point of closest approach and RC denotes the ring plane crossing. The emissions observed throughout the period of frequencies $\geq$ 60 kHz are due to freely propagating Saturn kilometric radiation (from Pedersen et al., 1981).

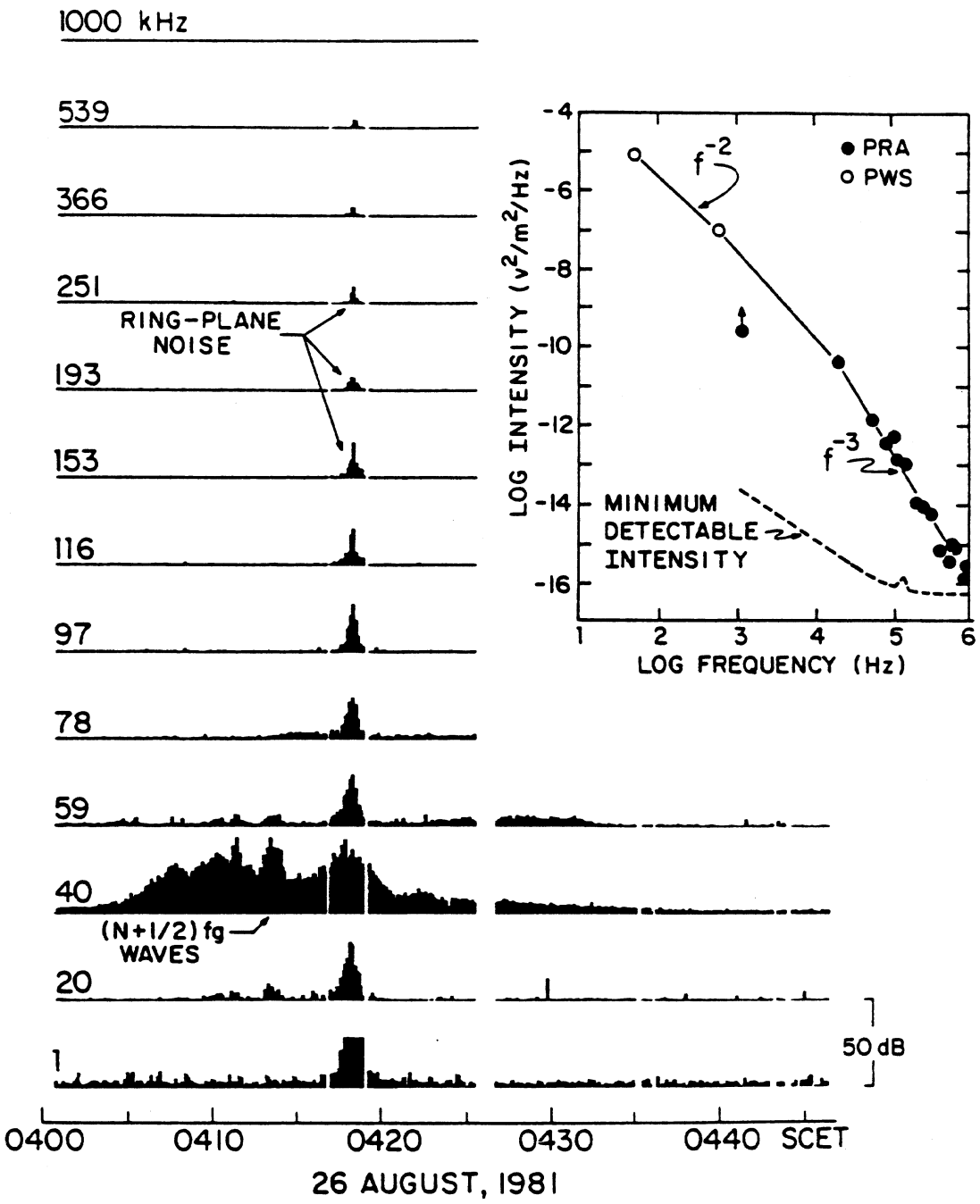

Figure 11: Relative intensity measured at 13 selected PRA–frequency channels around Voyager 2 – ring plane crossing just outside the G–ring. The insert shows the field intensity spectrum as measured at the peak of the ring plane event (0418 SCET) by the PRA–instrument and by two channels of the PWS–experiment (from Warwick et al., 1982).

inner to the outer side of the torus. This may be due to a heating of the cold electrons, a cooling of the hot, or a combination of the two processes.

Now the plasma waves, observed close to the Jovian magnetic equatorial plane outside the plasma torus, present the same characteristics as the plasma waves in the Io plasma torus, but for a plasma environment with $f_{pe} \gg f_{ce}$. This suggests that this two component plasma within the torus is not confined to the orbit of Io, but also forms a very extended tail, within which the source of free energy for the waves is provided by a loss cone distribution of the hot electrons.

These equatorially confined plasma waves might be the source of Jovian narrowband kilometric radiation (Kaiser and Desch, 1980), as it has been suggested by Kurth et al. (1981). Indeed, accordingly to Kaiser and Desch the source region for this radiation near 100 kHz, emitted in a very narrow bandwidth ($<$ 40 kHz), could lie near the equator outside the Io Plasma torus near 8–9 R_J.

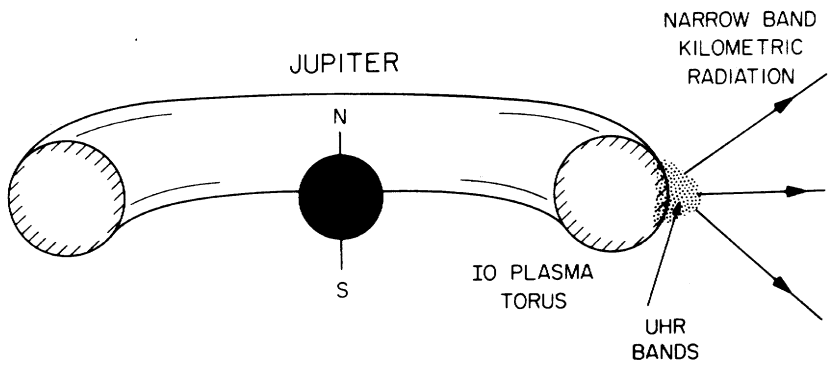

Figure 12: A schematic representation showing a hypothetical generation region of narrowband kilometric radiation in the outside equatorial tail region of the Io plasma torus, where LF – plasma waves are detected (from Kurth et al., 1981).

Kurth et al. (1981) have drawn analogies between this Jovian kilometric radiation (nKOM) and the terrestrial escaping continuum radiation. Both kinds of radiation could be generated by intense electrostatic waves near the local upper hybrid resonance frequency in the source region. Similarly as the terrestrial continuum radiation is generated just outside the dawn plasmapause, particularly near the equator, the source of Jovian nKOM might be situated at the outer edge of the plasma torus (Figure 12).

In the same way, the plasma waves observed around Saturn's ring plane might be the origin of the narrowbanded emission in the same frequency range interpreted as escaping continuum radiation ((2) on Fig. 10).

4 Conclusion

We have described the various kinds of plasma waves in the Jovian and Saturnian magnetospheres, as observed by the Voyager Planetary Radio Astronomy experiments. We

have shown that the PRA–observations contribute in an important way to interprete low frequency plasma wave phenomena above $\sim$ 20 kHz.

Presently, we are looking forward to the Voyager 2 encounter with Uranus (January 1986). The detection of auroral hydrogen Lyman–Alpha emissions from Uranus (Clarke, 1982) is a strong indication of the existence of a magnetosphere around the planet. No radioemission has been detected yet (October 1984) by the PRA–instrument. The future observations of the nature and the location of plasma waves within a possible Uranian magnetosphere by the PWS and the PRA – experiments will be important for understanding the physics of a hitherto unknown kind of magnetosphere: the pole–on magnetosphere (Siscoe, 1971).

5 References

Aubier, M. G., N. Meyer–Vernet, and B. M. Pedersen, Shot Noise from Grain and Particle impacts in Saturn's Ring Plane, *Geophys. Res. Lett.*, **10**, 5, 1983.

Birmingham, T. J., J. K. Alexander, M. D. Desch, R. F. Hubbard, and B. M. Pedersen, Observations of Electron Gyroharmonic Waves and the Structure of the Io Torus, *J. Geophys. Res.*, **86**, 8497, 1981.

Clarke, J. T., Detection of Auroral Hydrogen Lyman–Alpha Emissions from Uranus, *Astrophys. J.*, **263**, L105, 1982.

Daigne, G., B. M. Pedersen, M. L. Kaiser, and M. D. Desch, Planetary Radio Astronomy Observations during the Voyager 1 Titan Flyby, *J. Geophys. Res.*, **87**, 1405, 1982.

Gough, M. P., P. J. Christiansen, G. Martelli, and E. J. Gershuny, Interaction of Electrostatic Waves with warm Electrons at the geomagnetic Equator, *Nature*, **279**, 515, l979.

Gurnett, D. A. and F. L. Scarf, Plasma Waves in the Jovian Magnetosphere, in *Physics of the Jovian Maqnetosphere*, edited by A. J. Dessler, Cambridge University Press, pp. 285-316, 1983.

Kaiser, M. L. and M. D. Desch, Narrow–band Jovian Kilometric Radiation: A New Radio Component, *Geophys. Res. Lett.*, **7**, 389, 1980.

Kaiser, M. L., M. D. Desch, W. S. Kurth, A. Lecacheux, F. Genova, B. M. Pedersen, and D. R. Evans, Saturn as a Radio Source, in *Saturn*, edited by T. Gehrels and M. S. Matthews, The University of Arizona Press, Tucson, Arizona, pp. 378-416, 1984.

Kurth, W. S., D. D. Barbosa, D. A. Gurnett, and F. L. Scarf, Electrostatic Waves in the Jovian Magnetosphere, *Geophys. Res. Lett.*, **7**, 57, 1980.

Kurth, W. S., D. A. Gurnett, and R. R. Anderson, Escaping Nonthermal Continuum Radiation, *J. Geophys. Res.*, **86**, 5519, 1981.

Kurth, W. S., F. L. Scarf, D. A. Gurnett, and D.D. Barbara, A Survey of Electrostatic Waves in Saturn's Magnetosphere, *J. Geophys. Res.*, **88**, 8959, 1983.

McNutt, Jr., R. L., J. W. Belcher, and H. S. Bridge, Positive Ion Observations in the Middle Magnetosphere of Jupiter, *J. Geophys. Res.*, **86**, 8319, 1981.

Neubauer, F. M., D. A. Gurnett, J. D. Scudder, and R. E. Hartle, Titan's Magnetospheric Interaction, in *Saturn*, edited by T. Gehrels and M. S. Matthews, The University of Arizona Press, Tucson, Arizona, pp. 760-787, 1984.

Pedersen, M. B., M. G. Aubier, and J. K. Alexander, Low–frequency plasma waves near Saturn, *Nature*, **292**, 714, 1981.

Scarf, F. L., L. A. Frank, D. A. Gurnett, L. J. Lanzerotti, A. Lazarus, and E. C. Sittler Jr., Measurements of Plasma, Plasma Waves and Suprathermal Charged Particles in Saturn's inner Magnetosphere, in *Saturn*, edited by T. Gehrels and M. S. Matthews, The University of Arizona Press, Tucson, Arizona, pp. 318-353, 1984.

Scarf, F. L. and D. A. Gurnett, A Plasma Wave Investigation for the Voyager Mission, *Space Sci. Rev.*, **21**, 289, 1977.

Scarf, F. L., D. A. Gurnett, W. S. Kurth, and R. L. Poynter, Voyager Plasma Wave Measurements at Saturn, *J. Geophys. Res.*, **88**, 8971, 1983.

Scudder, J. D., E. C. Sittler Jr., and H. S. Bridge, A Survey of the Plasma Electron Environment of Jupiter: A View from Voyager, *J. Geophys. Res.*, **86**, 8157, 1981.

Siscoe, G. L., Two Magnetic Tail Models for Uranus, *Planet. Space Sci.*, **19**, 483, 1971.

Warwick, J. W., J. B. Pearce, R. G. Peltzer, and A. . Riddle, Planetary Radio Astronomy Experiment for Voyager Missions, *Space Sci. Rev.*, **21**, 309, 1977.

Warwick, J. W., J. B. Pearce, A. C. Riddle, J. K. Alexander, M. D. Desch, M. L. Kaiser, J. R. Thieman, T. D. Carr, S. Gulkis, A. Boischot, C. C. Harvey, and B. M. Pedersen, Voyager 1 Planetary Radio Observations near Jupiter, *Science*, **204**, 995, 1979a.

Warwick, J. W., J. B. Pearce, A. C. Riddle, J. K. Alexander, M. D. Desch, M. L. Kaiser, J. R. Thieman, T. D. Carr, S. Gulkis, A. Boischot, Y. Leblanc, B. M. Pedersen, and D. H. Staelin, Planetary Radio Astronomy Observations from Voyager 2 near Jupiter, *Science*, **206**, 991, 1979b.

Warwick, J. W., J. B. Pearce, D. R. Evans, T. D. Carr, J. J. Schauble, J. K. Alexander, M. L. Kaiser, M. D. Desch, B. M. Pedersen, A. Lecacheux, G. Daigne, A. Boischot, and C. H. Barrow, Planetary Radio Astronomy Observations from Voyager 1 near Saturn, *Science*, **212**, 239, 1981.

Warwick, J. W., D. R. Evans, J. H. Romig, J. K. Alexander, M. D. Desch, M. L. Kaiser, M. Aubier, Y. Leblanc, A. Lecacheux, and P. M. Pedersen, Planetary Radio Astronomy Observations from Voyager 2 near Saturn, *Science*, **215**, 582, 1982.

Discussion

Question:

Are there particle density differences between the Jovian daytime and nighttime observations? The Voyager spacecraft was in the Io torus at two different local times.

Pedersen:

You have seen that during nighttimes there are lower densities, so it seems that there is no symmetry between daytime and nighttime.